Optimal Design of Sparse MIMO Arrays for Near-Field Ultrawideband Imaging

M. Burak Kocamis and Figen S. Oktem
Department of Electrical and Electronics Engineering,
Middle East Technical University, 06800 Cankaya, Ankara, Turkey
Email: {e174135,figeno}@metu.edu.tr

***Abstract*—Near-field ultrawideband imaging is a promising remote sensing technique in various applications such as airport security, surveillance, medical diagnosis, and through-wall imaging. Recently, there has been increasing interest in using sparse multiple-input-multiple-output (MIMO) arrays to reduce hardware complexity and cost. In this paper, based on a Bayesian estimation framework, an optimal design method is presented for two-dimensional MIMO arrays in ultrawideband imaging. The optimality criterion is defined based on the image reconstruction quality obtained with the design, and the optimization is performed over all possible locations of antenna elements using an algorithm called clustered sequential backward selection algorithm. The designs obtained with this approach are compared with that of some commonly used sparse array configurations in terms of image reconstruction quality for various noise levels.**

I. Introduction

Near-field ultrawideband imaging systems are emerging array-based systems for various applications such as airport security, surveillance, through-wall imaging and medical diagnosis [1]–[4]. In these systems, down-range and cross-range resolutions are determined by the frequency bandwidth and size of the antenna arrays. In the classical two-dimensional designs, element spacing is chosen as at most half of the center wavelength to eliminate undesired grating lobes. As a result, in applications demanding high-resolution, classical (non-sparse) planar arrays require high hardware complexity and cost.

To reduce this complexity and cost, recently, there has been increasing interest in using sparse multiple-input-multiple-output (MIMO) arrays in ultrawideband radar imaging applications. Many such sparse MIMO topologies have been suggested and tested for this purpose [5]–[11]. However, none of these designs have been optimal in terms of minimizing the image reconstruction error. In fact, in [5]–[7], the arrays have been designed by imposing some constraints on the desired beam pattern. In [8]–[11], the arrays have been designed based on some desired properties of the virtual arrays such as uniformity and minimal element shadowing. However, a systematic approach to the optimal design of MIMO arrays has not been developed from an inverse theoretic perspective which takes into account the quality of the reconstructed images obtained with the design.

In this paper, we present an approach for the optimal design of two-dimensional MIMO arrays based on a Bayesian framework. The problem of image reconstruction from MIMO measurements is formulated as a maximum posterior estimation problem. The optimality criterion is then defined based on the resulting image reconstruction errors obtained with the design. Design optimization is performed over all possible locations of antenna elements using the clustered sequential backward selection (CSBS) algorithm [12]. The algorithm starts with an initial antenna configuration and reaches the desired number of antenna elements by iteratively reducing the antenna elements based on the optimality criterion.

The performance of the developed approach is illustrated for a microwave imaging application. Design optimization is performed using two different initial array configurations, namely a uniform and a random configuration. The performance of the designs obtained with the CSBS algorithm is compared with the commonly used sparse arrays [8] such as Mills cross. Numerical results illustrate that CSBS-based designs outperform the MIMO topologies suggested earlier in terms of image reconstruction quality and under various different noise levels. Furthermore, it is observed that the approach yields designs with more uniform virtual arrays than that of other designs. A preliminary version of this approach was presented in [13].

II. Observation Model

For near-field imaging systems, a discrete model that relates the MIMO measurements to the discretized reflectivity distribution of the scene can be expressed as follows [4]:

$$y(x_T, x_R, z_T, z_R, k) = \sum_{x,y,z} \frac{1}{4\pi d_T d_R} f(x,y,z) p(k) e^{-jkd_T} e^{-jkd_R}. \quad (1)$$

Here $y(x_T, x_R, z_T, z_R, k)$ denotes the measurement obtained using the transmitter located at $(x_T, 0, z_T)$ and the receiver located at $(x_R, 0, z_R)$. The measurements are expressed in the temporal Fourier domain with f denoting the frequency and $k = 2\pi f/c$ denoting the frequency-wavenumber. The three-dimensional reflectivity distribution of the scene is denoted by $f(x,y,z)$. Moreover, $p(k)$ represents the Fourier transform of the transmitted pulse, and d_T and d_R respectively denote the distances of the corresponding transmitter and receiver antennas to the voxel at (x,y,z):

$$d_T = \sqrt{(x_T - x)^2 + y^2 + (z_T - z)^2}, \quad (2)$$

$$d_R = \sqrt{(x_R - x)^2 + y^2 + (z_R - z)^2}. \quad (3)$$

ISBN 978-0-9928626-7-1 © EURASIP 2017

The discrete model in Eqn. (1) can be rewritten in matrix-vector form as follows:

$$y = Af + w, \tag{4}$$

where f is the scene reflectivity vector, y is the measurement vector, w is the noise vector, and A is the observation matrix. Using lexicographic ordering, the scene reflectivity values and measurements are respectively converted to column vectors f and y. The matrix A is a rectangular matrix that describes the linear relation between the reflectivity and measurement vectors. Using Eqn. (1), the (i,j)th element of the observation matrix can be expressed as follows:

$$A_{i,j} = \frac{p(k)e^{-jkd_T}e^{-jkd_R}}{4\pi d_T d_R}, \tag{5}$$

Here i is the measurement index; that is, for each measurement, it indicates the locations of the transmitting and receiving antennas, and the frequency used. Moreover, j represents the corresponding voxel in the scene reflectivity function.

As is observed from the above equation, (i,j)th element of the observation matrix indicates the contribution of the jth voxel to the ith measurement. Hence, the total number of rows is equal to the length of the measurement vector, and the number of columns is equal to the length of the reflectivity vector. Denoting the number of receiver antennas, transmitter antennas, frequency steps, and reflectivity voxels as M, T, F, and N, respectively, the size of the matrix A is given by $MTF\times N$. Moreover, the size of the voxels in the reflectivity function is determined based on the desired down-range and cross-range resolutions of the system.

III. Optimal Design Method

We now present an approach for the optimal design of two-dimensional MIMO arrays based on a Bayesian framework. First the problem of image reconstruction from MIMO measurements is formulated as a maximum posterior estimation (MAP) problem, and then the optimality criterion for the design is defined based on the resulting image reconstruction errors.

In the MAP framework, the reflectivity and noise vectors are assumed to be complex Gaussian distributed as follows:

$$w \sim \mathit{CN}(0, \Sigma_w), \quad f \sim \mathit{CN}(f_0, \Sigma_f), \tag{6}$$

where Σ_w denotes the covariance matrix of the noise vector, and f_0 and Σ_f respectively denote the mean and covariance matrix of the reflectivity vector. Then the MAP estimate of the scene reflectivity vector has a closed-form given by

$$\hat{f}_{\mathrm{MAP}} = f_0 + (A^H\Sigma_w^{-1}A + \Sigma_f^{-1})^{-1}A^H\Sigma_w^{-1}(y - Af_0), \tag{7}$$

where superscript $(.)^H$ represents the Hermitian of a matrix. In particular, if the noise is assumed as independent and identically distributed (i.i.d.) with variance σ_w^2, and the covariance matrix of the reflectivity vector has the form $\Sigma_f = (1/\gamma^2)(L^TL)^{-1}$, the MAP estimate becomes equivalent to the Tikhonov regularized least-squares solution given by

$$\hat{f}_{\mathrm{Tik}} = f_0 + (A^HA + \lambda L^TL)^{-1}A^H(y - Af_0), \tag{8}$$

where $\lambda = (\gamma\sigma_w)^2$ is the equivalent regularization parameter. One possible choice for the transformation L is the discrete derivative operator.

The error covariance matrix for this MAP estimate is given by [14]

$$\Sigma_e = (A^H\Sigma_w^{-1}A + \Sigma_f^{-1})^{-1}. \tag{9}$$

We define the optimality criterion based on the image reconstruction errors resulting from this estimation. After choosing this criterion, the design optimization is performed using the clustered sequential backward selection (CSBS) algorithm developed in [12] for this statistical framework. It is possible to define various different optimality criteria based on Σ_e [12]. Here, we define the optimality criterion as the mean square error (MSE), i.e. the trace of the error covariance matrix:

$$\mathrm{Cost}(A) = \mathrm{Tr}(\Sigma_e) = \sum_{i=1}^{N}(\Sigma_e)_{ii}, \tag{10}$$

For a given number of antenna elements, the goal in the optimal design is to obtain an array configuration that minimizes this cost function. For this purpose, the optimization starts with an initial antenna configuration with large number of antenna elements, and then the antennas are successively reduced using the CSBS algorithm until the desired number of elements is reached. The reduction of the antenna elements corresponds to the elimination of the respective rows from the observation matrix. The optimality criterion is used to identify which rows to eliminate. That is, at each iteration, the cost function of the design resulting from the removal of each antenna element is calculated, and the one that yields the minimum cost value is removed from the current design. Equivalently, corresponding rows from the observation matrix are eliminated. This process continues until the desired number of antennas is reached for the design.

In order to reduce the computational complexity, the cost function can be equivalently replaced with the following [12]:

$$\Gamma \longleftarrow \Gamma \setminus k^* : k^* = \arg\min_{k\epsilon\Gamma} \sum_{i\epsilon\Pi_k} \frac{a_i\Sigma_e^2 a_i^H}{1 - a_i\Sigma_e a_i^H}, \tag{11}$$

where Γ contains the indices of the antenna elements in the current configuration, and k^* represents the index of the antenna element that is removed from the current configuration. Moreover, a_i shows the ith row of the observation matrix, Π_k contains the row numbers corresponding to the measurements related to the kth antenna. To compute this cost function, matrix Σ_e is required to be updated at each iteration using the current observation matrix A^Γ and Eqn. (9).

In order to analyze the computational complexity of the CSBS algorithm, recall that Σ_e and the summation in Eqn. (11) are required to be computed at each iteration. Computation of Σ_e involves matrix multiplication and inversion operations in Eqn. (9). Assuming that the number of rows in the updated matrix A^Γ is Q ($Q \leq MTF$), the computational complexity is $O(Q^2N + N^2Q)$ for the matrix multiplications and $O(N^3)$ for the matrix inversion. Since $Q \geq N$, the computational complexity of Σ_e calculation becomes $O(Q^2N)$. Moreover,

ISBN 978-0-9928626-7-1 © EURASIP 2017

if the sum of the receiver and transmitter antenna elements is denoted by P ($P = M + T$), then the computational complexity of the summation in Eqn. (11) is $O(N^2P)$. Hence, the computational complexity of one iteration becomes $O(Q^2N + N^2P)$. Since $Q \geq N$ and $Q \geq P$, computational complexity of one iteration can be expressed as $O(Q^2N)$.

IV. Simulation Scenario and Results

A. Scenario

To compare the image reconstruction quality of the CSBS-designed arrays with the commonly used sparse antenna arrays, a microwave imaging scenario is considered. The parameters used in this scenario are given in Table I.

TABLE I
SCENARIO PARAMETERS

Parameters	Value
Center Frequency (f_c)	11 GHz
Bandwidth (B)	16.7 GHz
Number of Frequency Steps (F)	7
Center Wavelength (λ_c)	2.73 cm

CSBS algorithm is applied to two different initial antenna configurations. As shown in Figure 1, the first one is a uniform planar array, and the second one is random and has uniformly distributed antennas. Initial array sizes are the same for both configurations; each is located between $-10\lambda_c$ to $10\lambda_c$ in x and z axes. Moreover, initial antenna configurations contain 242 antennas equally shared for receiver and transmitter antennas. The goal is to reduce the number of antennas to the desired number of 25 using the CSBS algorithm.

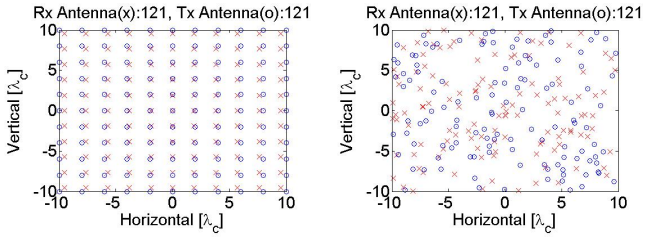

Fig. 1. Initial uniform antenna configuration (left), initial random antenna configuration (right).

In the uniform antenna configuration, the spacing between transmitter antennas is set to $\lambda_c/2$. In order to avoid overlapping of the virtual array elements, the spacing between receiver antennas is chosen different than $\lambda_c/2$. In fact, the ratio between the spacings of receiver and transmitter antennas is chosen as an irrational number of $3/\pi$, while keeping the size of the transmit and receive arrays close to each other .

In the simulations, a point scatterer is considered as in [8], and the distance from the point target to the antenna array is selected as $40\lambda_c$. The reflectivity cube of interest is divided into $19\times19\times3$ voxels in the x, z and y directions, respectively. The width of the reflectivity cube along x and z directions is same as that of the antenna array, and the voxel size is determined based on down-range and cross-range resolutions of the system. The point scatterer is at the center of this reflectivity cube. The elements of the observation matrix is calculated using Eqn. (5), and here $p(k)$ is taken as unity. For the observation noise w, i.i.d. complex Gaussian noise with $\sigma_w = 10^{-4}$ is used.

To compare the imaging performance of the CSBS-based arrays, Mills cross and curvilinear array topologies in [8] are considered. The observation matrix for these sparse arrays are calculated similarly using Eqn. (5). For each array configuration, the reflectivity vector is reconstructed using Tikhonov regularization as given in Eqn. (8), with λ chosen as the optimal regularization parameter and L chosen as the discrete derivative operator. Using the central slice of the reconstructed reflectivity cubes, the point-spread functions of all array topologies are compared.

B. Results

Figure 2 shows the array designs obtained by applying the CSBS algorithm to the initial antenna configurations of uniform and random arrays. Mills cross and curvilinear array designs from [8], used for comparison, are shown in Figure 3.

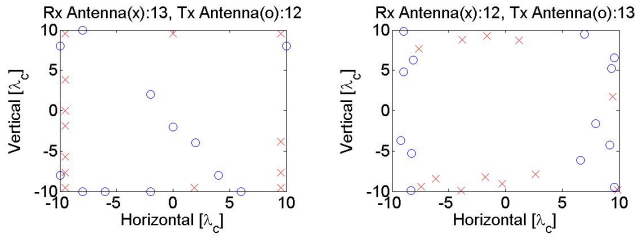

Fig. 2. Array design obtained with initially uniform antenna configuration (left), Array design obtained with initially random antenna configuration (right).

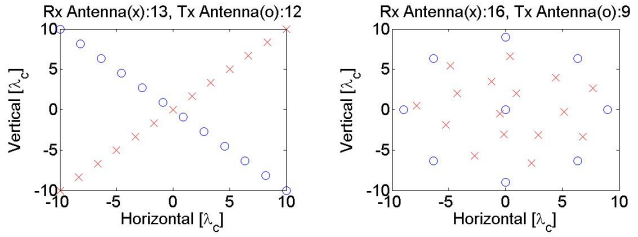

Fig. 3. Mills Cross array (left), curvilinear array (right)

For each design, the reflectivity cube is reconstructed from the measurements, and its central slice (that contains the point scatterer) is shown in Figure 4. Mean squared errors are also calculated for 100 Monte Carlo trials and their average is shown in Table II. As shown from the results in Figure 4 and Table II, CSBS-based designs outperform the earlier designs

ISBN 978-0-9928626-7-1 © EURASIP 2017

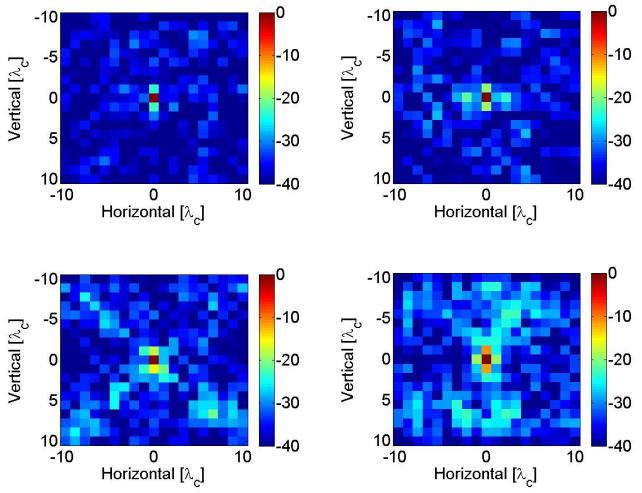

Fig. 4. Two dimensional reconstruction results in dB: for the design obtained with initially uniform array (upper left), for the design obtained with initially uniform array (upper right), for Mills cross array (bottom left), for curvilinear array (bottom right)

TABLE II
MSE VALUES FOR ALL ARRAY TOPOLOGIES FOR $\sigma_w = 10^{-4}$

Array Type	Average MSE
Design with initially uniform array	0.38
Design with initially random array	0.48
Mills cross	0.59
Curvilinear	0.69

suggested in the literature. They yield much cleaner point-spread functions with less sidelobes.

The performance of each design (in terms of MSE) is also shown in Figure 5 for varying noise standard deviation. It is observed that designs obtained with the developed approach always perform better for any SNR value, and at high SNRs curvilinear array outperforms Mills cross array, as consistent with the results of [8].

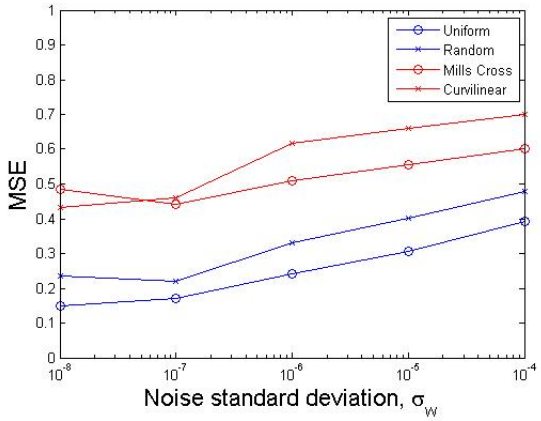

Fig. 5. MSE vs noise standard deviation for all topologies

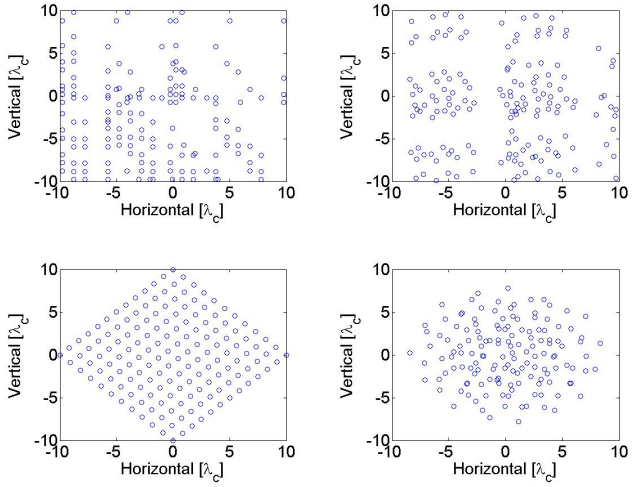

Fig. 6. Virtual arrays: for the design obtained with initially uniform array (upper left), for the design obtained with initially uniform array (upper right), for Mills cross array (bottom left), for curvilinear array (bottom right)

Moreover, in the literature, it has been proposed that the virtual array of an antenna configuration is related to the goodness of the design, and that the uniformity of the virtual array affects the imaging performance positively [15]. Figure 6 shows the virtual arrays of the all four designs. The virtual arrays of the CSBS-based designs also appear to be more uniform compared to the other two topologies. This is also consistent with the MSE results in Table II.

V. CONCLUSION

In this paper, an optimal design approach is presented for two-dimensional MIMO arrays used in near-field ultrawideband imaging. For image reconstruction, MAP estimation (equivalently, regularized least-squares) approach is considered, and the mean squared error (MSE) in the reconstruction is chosen as the optimality criterion for the design. Design optimization is performed over all possible locations of antenna elements using the CSBS algorithm. The performance of the developed approach is illustrated for a microwave imaging application. The results illustrate that the designs obtained with this approach outperform commonly used sparse array configurations in terms of image reconstruction quality for a wide range of SNR.

ACKNOWLEDGMENT

The problem studied in this paper is inspired by a project supported by ASELSAN A.S.

REFERENCES

[1] J. D. Taylor, *Ultrawideband Radar: Applications and Design*. CRC press, 2011, ch. 17.
[2] S. S. Ahmed *et al.*, "Advanced microwave imaging," *IEEE Microwave Mag.*, pp. 26–43, 2012.
[3] X. Zhuge and A. G. Yarovoy, "A sparse aperture MIMO-SAR-based UWB imaging system for concealed weapon detection," *IEEE Trans. on Geosci. and Remote Sensing*, pp. 509–518, 2011.
[4] ——, "Three-dimensional near-field MIMO array imaging using range migration techniques," *IEEE Trans. on Image Process.*, pp. 3026–3033, 2012.

[5] B. Yang *et al.*, "UWB MIMO antenna array topology design using PSO for through dress near-field imaging," in *Proc. German Microwave Conf.*, 2008, pp. 463–466.
[6] T. Savelyev *et al.*, "Comparison of UWB SAR and MIMO-based short-range imaging radars," in *Proc. European Radar Conf.*, 2009, pp. 109–112.
[7] Y. Liu *et al.*, "Reducing the number of elements in a linear antenna array by the matrix pencil method," *IEEE Trans. on Antennas and Propagation*, pp. 2955–2962, 2008.
[8] X. Zhuge and A. G. Yarovoy, "Study on two-dimensional sparse MIMO UWB arrays for high resolution near-field imaging," *IEEE Trans. on Antennas and Propagation*, pp. 4173–4182, 2012.
[9] K. Tan *et al.*, "A novel two-dimensional sparse MIMO array topology for UWB short-range imaging," *IEEE Antennas and Wireless Propagation Letters*, pp. 702–705, 2016.
[10] ——, "On sparse MIMO planar array topology optimization for UWB near-field high-resolution imaging," *IEEE Trans. on Antennas and Propagation*, pp. 989–994, 2017.
[11] X. Zhuge and A. Yarovoy, "Near-field ultra-wideband imaging with two-dimensional sparse MIMO array," in *Proc. European Conf. on Antennas and Propagation (EuCAP)*, 2010, pp. 1–4.
[12] B. Sharif and F. Kamalabadi, "Optimal sensor array configuration in remote image formation," *IEEE Trans. on Image Process.*, pp. 155–166, 2008.
[13] M. B. Kocamis and F. S. Oktem, "Optimal MIMO array configuration for ultrawideband microwave imaging," in *2017 25th Signal Processing and Communication Application Conference (SIU)*. IEEE, 2017.
[14] S. M. Kay, *Fundamentals of Statistical Signal Processing: Estimation Theory*, NJ, Upper Saddle River:Prentice Hall, 1993.
[15] K. Forsythe *et al.*, "Multiple-input multiple-output (MIMO) radar: Performance issues," in *Proc. IEEE 38th Asilomar Conf. on Signals, Syst. and Comput.*, 2004, pp. 310–315.

ISBN 978-0-9928626-7-1 © EURASIP 2017